

# Impact of Detergent on Biophysical Properties and Immune Response of the IpaDB Fusion Protein, a Candidate Subunit Vaccine against *Shigella* Species

Xiaotong Chen,<sup>a\*</sup> Shyamal P. Choudhari,<sup>a\*</sup> Francisco J. Martinez-Becerra,<sup>a\*</sup> Jae Hyun Kim,<sup>b</sup> Nicholas E. Dickenson,<sup>a\*</sup> Ronald T. Toth IV,<sup>b</sup> Sangeeta B. Joshi,<sup>b</sup> Jamie C. Greenwood II,<sup>a</sup> John D. Clements,<sup>c</sup> William D. Picking,<sup>a\*</sup> C. Russell Middaugh,<sup>b</sup> Wendy L. Picking<sup>a\*</sup>

Department of Microbiology and Molecular Genetics, Oklahoma State University, Stillwater, Oklahoma, USA<sup>a</sup>; Department of Pharmaceutical Chemistry, University of Kansas, Lawrence, Kansas, USA<sup>b</sup>; Department of Microbiology and Immunology, Tulane University School of Medicine, New Orleans, Louisiana, USA<sup>c</sup>

*Shigella* spp. are causative agents of bacillary dysentery, a human illness with high global morbidity levels, particularly among elderly and infant populations. *Shigella* infects via the fecal-oral route, and its virulence is dependent upon a type III secretion system (T3SS). Two components of the exposed needle tip complex of the *Shigella* T3SS, invasion plasmid antigen D (IpaD) and IpaB, have been identified as broadly protective antigens in the mouse lethal pneumonia model. A recombinant fusion protein (DB fusion) was created by joining the coding sequences of IpaD and IpaB. The DB fusion is coexpressed with IpaB's cognate chaperone, IpgC, for proper recombinant expression. The chaperone can then be removed by using the mild detergents octyl oligoxyethelene (OPOE) or *N,N*-dimethyldodecylamine *N*-oxide (LDAO). The DB fusion in OPOE or LDAO was used for biophysical characterization and subsequent construction of an empirical phase diagram (EPD). The EPD showed that the DB fusion in OPOE is most stable at neutral pH below 55°C. In contrast, the DB fusion in LDAO exhibited remarkable thermal plasticity, since this detergent prevents the loss of secondary and tertiary structures after thermal unfolding at 90°C, as well as preventing thermally induced aggregation. Moreover, the DB fusion in LDAO induced higher interleukin-17 secretion and provided a higher protective efficacy in a mouse challenge model than did the DB fusion in OPOE. These data indicate that LDAO might introduce plasticity to the protein, promoting thermal resilience and enhanced protective efficacy, which may be important in its use as a subunit vaccine.

Shigellosis, a severe dysenteric disease caused by *Shigella* spp., kills approximately 100,000 children under the age of 5 years each year, with ~90 million more being hospitalized and suffering adverse, long-term developmental effects from malnutrition associated with repeated diarrheal episodes (1). *Shigella* spp. are transmitted by the fecal-oral route, and only 10 to 100 organisms are required to cause an infection. Thus, most infections are associated with poor sanitation and contaminated water. There are four species of *Shigella* (*S. flexneri*, *S. sonnei*, *S. dysenteriae*, and *S. boydii*) that encompass ~50 unique serotypes across the genus, with atypeable serotypes frequently being identified. Thus, despite considerable efforts, a broadly protective, serotype-independent vaccine to prevent shigellosis is currently unavailable.

The type III secretion system (T3SS) is a common virulence factor among Gram-negative pathogens. The T3SS is used by *Shigella* spp. to promote inflammation by causing macrophage apoptosis and infection, as it induces internalization of bacteria into epithelial cells (2). Genes for the protein effectors of the T3SS that are responsible for host cell invasion are carried along with genes for the secretion apparatus on a 220-kb virulence plasmid. The effectors are translocated into the host cell via the type III secretion apparatus (T3SA) (3), which resembles a molecular needle and syringe, with a basal body anchoring the apparatus into the bacterial envelope, an external needle, and a needle tip complex (3). Because the structural proteins of the T3SS are highly conserved among *Shigella* species, they are potentially serotype-independent protective antigens. Indeed, two proteins of the needle tip complex, IpaD and IpaB, have proven to be protective antigens when

administered mucosally or parenterally in the mouse lethal pulmonary infection model (4–6).

While the identification of IpaD and IpaB as protective antigens was a major step forward, the target vaccination group is children of the developing world. A vaccine formulation containing two proteins, in addition to an adjuvant, may be prohibitively expensive. Recently, we have reduced the potential cost by creating a novel fusion protein composed of IpaD and IpaB (7). Al-

Received 7 August 2014 Returned for modification 9 September 2014

Accepted 26 October 2014

Accepted manuscript posted online 3 November 2014

**Citation** Chen X, Choudhari SP, Martinez-Becerra FJ, Kim JH, Dickenson NE, Toth RT, IV, Joshi SB, Greenwood JC, II, Clements JD, Picking WD, Middaugh CR, Picking WL. 2015. Impact of detergent on biophysical properties and immune response of the IpaDB fusion protein, a candidate subunit vaccine against *Shigella* species. *Infect Immun* 83:292–299. doi:10.1128/IAI.02457-14.

**Editor:** S. M. Payne

Address correspondence to Wendy L. Picking, [wendy.picking@ku.edu](mailto:wendy.picking@ku.edu).

\* Present address: Nicholas E. Dickenson, Department of Chemistry and Biochemistry, Utah State University, Logan, Utah, USA; Xiaotong Chen, Shyamal P. Choudhari, Francisco J. Martinez-Becerra, William D. Picking, and Wendy L. Picking, Department of Pharmaceutical Chemistry, University of Kansas, Lawrence, Kansas, USA.

Supplemental material for this article may be found at <http://dx.doi.org/10.1128/IAI.02457-14>.

Copyright © 2015, American Society for Microbiology. All Rights Reserved.

doi:10.1128/IAI.02457-14

though similar antibody titers to IpaD and IpaB were obtained when the DB fusion was administered intranasally, higher gamma interferon (IFN- $\gamma$ ) and interleukin-17A (IL-17A) responses, essential for protection against *Shigella* spp. (8), were observed with the fusion. Moreover, the DB fusion provided protection against *S. flexneri* 2457T, *S. sonnei*, and *S. dysenteriae*. The DB fusion has also been shown to be protective when administered parenterally (F. J. Martinez-Becerra, unpublished data).

Like IpaB, the DB fusion requires a detergent to release IpgC, the IpaB chaperone, from the coexpressed DB fusion/IpgC complex and to maintain solubility of the DB fusion after release (7). Initially, the mild detergent octyl oligoxyethelene (OPOE) was used, based on its success in maintaining the structure and solubility of IpaB. As a less expensive alternative, the detergent *N,N*-dimethyldodecylamine *N*-oxide solution (LDAO) was then examined and found to impart distinct characteristics to the DB fusion, including thermal resilience and plasticity, as well as protective efficacy. Here, we describe these characteristics as part of the preformulation characterization of the DB fusion, using biophysical techniques and the collective data, which we illustrate with three-index empirical phase diagrams (EPDs) to depict the overall structural integrity and conformational stability of the protein under different conditions.

## MATERIALS AND METHODS

**Protein purification and sample preparation.** Construction of the plasmid containing the gene for the DB fusion and the protein purification methods have been described previously (7). Briefly, DB/pET28b+ipgC/pACYCDuet-1//Tuner(DE3) cells were grown in autoinduction medium. The bacteria were collected by centrifugation, resuspended in immobilized metal affinity chromatography (IMAC) binding buffer containing 0.2 mM 4-(2-aminoethyl)benzenesulfonyl fluoride hydrochloride, and lysed, and the suspension was clarified. The DB fusion/IpgC complex was purified by IMAC, hydrophobic interaction chromatography, and finally anion-exchange chromatography (7). A second IMAC purification was then performed using the detergent OPOE (0.5% [vol/vol]) in the wash and elution buffers to remove the chaperone from the DB fusion and maintain the DB fusion in solution, respectively. Alternatively, the detergent LDAO (0.05% [vol/vol]) was also used to remove the chaperone and maintain the DB fusion in soluble form. The critical micelle concentrations (CMCs) for OPOE and LDAO are 0.3% and 0.02%, respectively. A lower concentration of LDAO was used, since that amount was sufficient for chaperone release, solubility of the DB fusion, and lack of impact of higher concentrations on biophysical characteristics, including thermal resilience. Fractions were analyzed by SDS-PAGE and stored at  $-80^{\circ}\text{C}$ . For biophysical studies, the DB fusion was dialyzed into 20 mM citrate-phosphate (CP) buffer with an ionic strength of 0.15 at the desired pH with either 0.5% (vol/vol) OPOE or 0.05% (vol/vol) LDAO. Finally, the protein was filtered through 0.22- $\mu\text{m}$  filters, and the concentration was adjusted to 0.1 mg/ml. For simplicity, the DB fusion in OPOE is abbreviated as the OPOE-DB fusion. Similarly, the DB fusion in LDAO is abbreviated as the LDAO-DB fusion. These abbreviations are consistent with the nomenclature for IpaB in each detergent (9) but do not denote a covalent linkage of either of the detergents to the protein.

**Analytical ultracentrifugation.** DB fusion proteins were purified, and the concentrations were adjusted to 8  $\mu\text{M}$  in phosphate-buffered saline (PBS; pH 7.4) containing 0.5% OPOE or 0.05% LDAO and covalently cross-linked by the addition of the amine-reactive cross-linker dithiobis(succinimidylpropionate). The reaction was maintained for 15 min at room temperature and quenched with 70 mM Tris-HCl (pH 7.4). The detergent was then removed by dialysis into PBS (pH 7.4). Sedimentation velocity with analytical ultracentrifugation (SV-AUC) experiments were performed with an Optima XL-I analytical ultracentrifuge (Beckman

Coulter, Fullerton, CA) equipped with a scanning UV-visible optical system. Samples and the reference were loaded into Beckman charcoal-Epon two-sector cells with 12-mm sapphire windows. All experiments were conducted at  $20^{\circ}\text{C}$  with a rotor speed of 40,000 rpm and with detection at 280 nm.

The AUC data were analyzed using Sedfit (10). The default partial specific volume of 0.73 ml/g was used in the analysis. Values for buffer density and viscosity were calculated using Sednterp (11) and were based on the buffer composition. A continuous size distribution  $[c(s)]$  was used, with 280 scans. A range of 0 to 15 Svedberg units was used for the LDAO-DB fusion, and a range of 0 to 50 Svedberg units was used for the OPOE-DB fusion, after verifying that there was no material sedimenting outside these ranges. A resolution of 400 points per distribution was used, with a confidence level of 0.95. Best-fit frictional ratios of 1.43 and 1.51 were used for the LDAO-DB fusion and OPOE-DB fusion, respectively. Baseline, radial-independent noise and time-independent noise were also fit, while the meniscus and bottom positions were set manually.

The monomer peak was assigned by comparing the experimentally observed sedimentation coefficients to the maximum theoretical sedimentation coefficient of the monomer, calculated based on the molecular weight, as described by Lebowitz et al. (12). The oligomeric states of other observed species were determined by dividing the experimentally observed sedimentation coefficient of the oligomer by that of the monomer, as described by García de la Torre and Bloomfield (13). The percent mass was assigned based on integration of the  $c(s)$  peaks by using Origin (OriginLab, Northampton, MA). The sedimentation coefficients reported are peak maxima.

**Far-UV CD spectroscopy.** Far-UV circular dichroism (CD) spectra were collected as previously described (9). Briefly, CD spectra of DB fusion in citrate-phosphate buffer with detergent at pH 3.0 to 8.0 were measured using a Jasco J-815 CD spectrometer equipped with a six-position Peltier temperature controller coupled with six 0.1-cm-path-length cuvettes. The spectra were collected from 260 to 190 nm at  $10^{\circ}\text{C}$  with a scanning speed of 50 nm/min, a 1.0-nm spectral resolution, and a 2-s data integration time. All spectra are averages of three measurements. Thermal melts were measured by collecting the CD signal at 222 nm every  $2.5^{\circ}\text{C}$ , with the temperature increasing from  $10^{\circ}\text{C}$  to  $90^{\circ}\text{C}$  via a temperature ramp rate of  $15^{\circ}\text{C}/\text{h}$ . Two repeats were obtained, and all three sets of signal data were converted into molar ellipticity and plotted (Jasco Spectral Manager and Origin 8.6).

**Intrinsic Trp fluorescence.** Intrinsic tryptophan (Trp) fluorescence spectra of the DB fusion were obtained with a Photon Technology International (PTI) spectrofluorometer (Birmingham, NJ) equipped with a turreted 4-position Peltier-controlled cell holder (9). Trp residues were excited at a wavelength of 295 nm, and the emission spectra were collected from 300 to 400 nm with a step size of 1 nm and a 0.5-s integration time. Samples in citrate-phosphate buffers (pH 3 to 8) in the presence of 0.5% OPOE or 0.05% LDAO at various pHs (3 to 8) were loaded into quartz cuvettes with a 1-cm path length, and the emission spectra were acquired from 10 to  $85^{\circ}\text{C}$  with an increase of  $2.5^{\circ}\text{C}$ . The samples were equilibrated for 3 min prior to each measurement. The excitation and emission slit widths were maintained at 3 nm throughout the study. Three readings were taken for each sample, and a spectrum for blank buffer at each pH was subtracted from the sample spectra. Peak positions were obtained using Origin software and a mean spectral center-of-mass (MSM) method. The emission peak position calculated by the MSM method accurately reflects spectral changes but not the actual value, with 10 to 14 nm shifts occurring during the analysis. Static light scattering at 295 nm was measured simultaneously by using a second detector placed  $180^{\circ}$  from the fluorescence photomultiplier.

**Three-index empirical phase diagram.** Data acquired via multiple techniques, including far-UV CD melts, intrinsic Trp fluorescence, and static light scattering, were combined and constructed into a three-index EPD, which provides a colored representation of overall structural integrity and conformational stability of a protein as a function of pH and

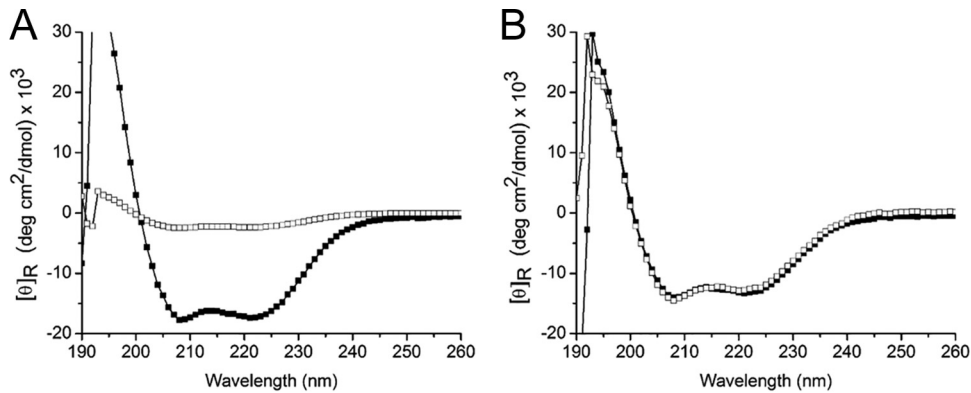


**FIG 1** Far-UV circular dichroism spectra of the DB fusion before and after thermal melt. The DB fusion in PBS (pH 7.0) with 0.5% OPOE (A) or 0.05% LDAO (B) was used to obtain far-UV CD spectra at 10°C before (■) and after (□) thermal unfolding.

temperature (14). The three techniques indicate changes in a protein's secondary, tertiary, and quaternary structures. Briefly, each data set obtained from different methods was normalized into a structural index ranging from 0 to 1. Each structural index was then mapped to an RGB color component: red, green, and blue were assigned to the secondary, tertiary, and quaternary structure, respectively.

**Immunogenicity.** All animal experiments were approved by the Oklahoma State University Institutional Animal Care and Use Committee. Mice ( $n = 10$  per group) were immunized with 20  $\mu$ g of OPOE-DB fusion or LDAO-DB fusion admixed with the mucosal adjuvant double-mutant labile toxin (dmLT; 2.5  $\mu$ g) from enterotoxigenic *Escherichia coli*. Vaccines were delivered intranasally three times, on days 0, 14, and 28. Blood samples were collected at days 0, 14, 28, 42, and 56, and serum was separated and tested for antibodies against IpaB and IpaD as described previously (7). Splenocytes were obtained from immunized mice at day 56 and stimulated with 5  $\mu$ g/ml IpaB or IpaD for 48 h. Supernatants were collected, and IL-17A levels were measured using an IL-17A enzyme-linked immunosorbent assay (ELISA) kit (R&D Systems, Minneapolis, MN).

***Shigella flexneri* challenge.** Immunized mice were challenged with *S. flexneri* 2457T as previously described (7). Briefly, bacteria were grown at 37°C with agitation until the  $A_{600}$  reached  $\sim 1$ . Bacteria were centrifuged and resuspended in PBS. On day 56, mice were challenged by delivering  $1.6 \times 10^7$  CFU of *Shigella* intranasally in a volume of 30  $\mu$ l. Weight loss and health scores were monitored for 14 days. Survival was analyzed using log rank tests.

## RESULTS

**The DB fusion can be stably purified in the detergent LDAO.** While the detergent OPOE was originally employed to release IpaB from its cognate chaperone, IpgC, and to maintain IpaB in solution, it does not have a defined molecular structure, which makes it suboptimal for initiation of crystallographic studies of IpaB. LDAO, which has a defined molecular weight, was used as a substitute and found to release IpaB and maintain it in a soluble state (9). Since LDAO is substantially less expensive and has a GRAS (generally regarded as safe) profile, which is helpful for vaccine development, we used LDAO in the DB fusion purification scheme and compared the characteristics of the LDAO-DB fusion to those of the OPOE-DB fusion. After the DB fusion/IpgC complex was purified, LDAO was added to the protein solution in binding buffer and loaded onto an IMAC column. The IpgC passed through the column, while the DB fusion remained bound to the resin and was eluted with increased imidazole with 0.05% LDAO (data not shown). At this concentration of LDAO, the DB fusion was found to be maintained in a soluble form, with no

aggregation detected visibly or by dynamic light scattering (data not shown).

**The DB fusion exhibits unique properties that are detergent dependent.** Unexpectedly, LDAO imparted characteristics to IpaB that were unique compared to OPOE, including thermal resilience and a switch from a tetrameric to monomeric oligomerization state (9). Thus, we assessed these characteristics in the DB fusion in PBS (pH 7.0). Regardless of the detergent, the CD spectrum of the DB fusion exhibited the typical double minima at 208 and 222 nm, which is expected from a highly  $\alpha$ -helical protein. After the OPOE-DB fusion or LDAO-DB fusion was subjected to an increase in temperature during a CD thermal melt analysis up to 90°C and cooled back to 10°C, the obtained CD spectra of the proteins were quite different (Fig. 1). The secondary structure of the OPOE-DB fusion was partially lost (Fig. 1A), with the protein now forming visible protein aggregates in the cuvette. In contrast, the spectrum of the LDAO-DB fusion after thermal melting was superimposable upon the spectrum prior to the thermal stress, suggesting that the protein recovered its secondary structure. While this property was also seen for IpaB (9) and IpaD (S. P. Choudhari and X. Chen, unpublished data), LDAO does not confer thermal resilience to all proteins. Bovine serum albumin completely unfolded and did not refold after high temperatures in either OPOE (data not shown) or LDAO (see Fig. S1 in the supplemental material). Although the LDAO concentration was 1/10 that of the OPOE concentration, it remained above the CMC of LDAO. Thus, the effect that LDAO has with 1/10 the concentration of OPOE is quite remarkable. At the lower concentration of OPOE, to mimic the LDAO concentration, the DB fusion forms aggregates. At higher concentrations of LDAO, no change in parameters was seen (data not shown).

To assess the oligomerization state of the DB fusion in each detergent, SV-AUC was conducted (Table 1; see also Fig. S2 in the supplemental material). Since the detergents interfered with the AUC measurements, the OPOE-DB fusion and LDAO-DB fusion were cross-linked, dialyzed into PBS, subjected to AUC, and analyzed by using the  $c(s)$  model. In the OPOE-DB fusion sample, a monomer peak was observed at 5.01 Svedberg units and a dimer peak was observed at 7.64 Svedberg units (Table 1). The most dominant peak in the distribution was a single peak containing both trimer and tetramer species, with a maximum at 11.15 Svedberg units (tetramer) and a shoulder at 9.80 Svedberg units

TABLE 1 SV-AUC results for DB fusion peak species in the presence of LDAO or OPEO

Detergent present and peak species	Sedimentation coefficient (Svedberg units) <sup>a</sup>	Relative % of mass <sup>b</sup>
With LDAO		
Fragment	3.19 ± 0.0037	15 ± 0.39
Monomer	4.82 ± 0.0016	54 ± 0.53
Dimer	7.03 ± 0.0043	26 ± 0.82
Trimer	9.60 ± 0.017	6 ± 0.75
With OPOE		
Monomer	5.01 ± 0.0072	16 ± 0.66
Dimer	7.64 ± 0.0040	9 ± 0.072
Trimer and tetramer	11.15 ± 0.010	45 ± 1.39
Hexamer	15.29 ± 0.0050	5 ± 1.51
Octamer	17.67 ± 0.018	3 ± 0.90
Higher-order aggregates	22.43 ± 0.021	6 ± 1.81
	25.19 ± 0.017	11 ± 3.31
	34.84 ± 0.041	2 ± 0.60
	41.23 ± 0.048	1 ± 0.30

<sup>a</sup> Values are means ± standard errors; errors for sedimentation coefficients were determined using Monte-Carlo simulation with a 95% confidence interval.

<sup>b</sup> The relative percentages of mass that could be attributed to each DB fusion species are expressed as means ± standard errors; errors were determined based on the root mean square deviation of the fit.

(trimer) (see Fig. S2). Additional minor aggregate peaks were also observed, including a hexamer (15.29 Svedberg units), octamer (17.67 Svedberg units), and other higher-order species. The LDAO-DB fusion sample also contained some degradation products, which were represented as a peak with a sedimentation coefficient of 3.19 Svedberg units, along with the dominant monomer peak at 4.82 Svedberg units and minor populations of dimer (7.03-Svedberg-unit) and trimer (9.6-Svedberg-unit) peaks (Table 1). Thus, as seen for IpaB, LDAO does not promote stable oligomerization of the DB fusion.

**The DB fusion in LDAO maintains the secondary structure under stress.** Far-UV CD spectroscopy was used to investigate secondary structure content and stability across a pH range from 3 to 8. CD spectra of the OPOE-DB fusion and LDAO-DB fusion at 10°C (see Fig. S3 in the supplemental material) displayed double minima at 208 and 222 nm; again, this was consistent with the presence of a significant  $\alpha$ -helical structure across the pH range examined. A slight decrease in CD signal was observed for the OPOE-DB fusion under low-pH (pH 3, 4, and 5) conditions compared to that at neutral pH, indicating that the average structure of the protein at acidic pH was slightly altered, and little pH dependence was seen with the LDAO-DB fusion sample.

The CD thermal melts of both samples (Fig. 2A and D) indicated a reduction in  $\alpha$ -helical content, since the molar ellipticities at 222 nm decreased as the temperature increased. The degree of change in molar ellipticities, however, was detergent dependent.

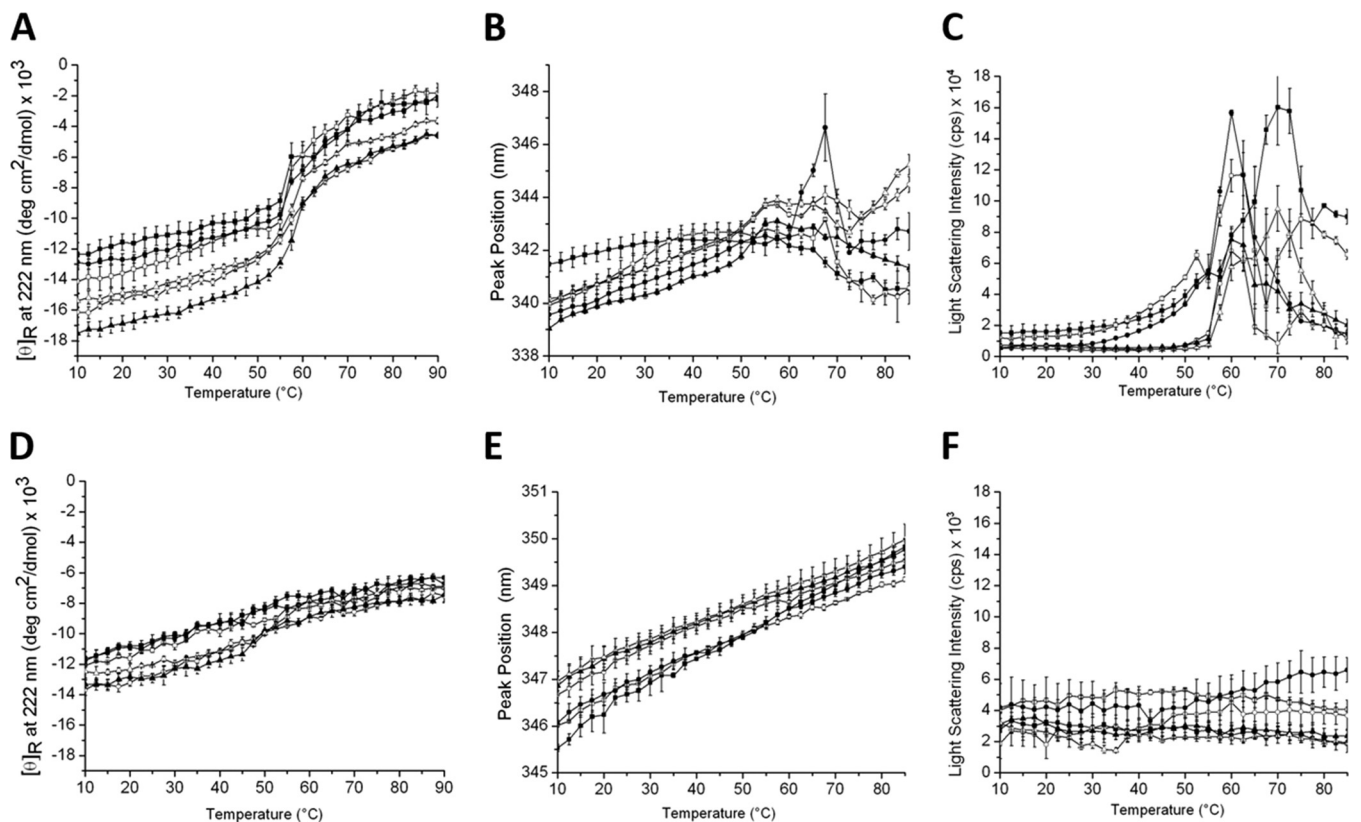
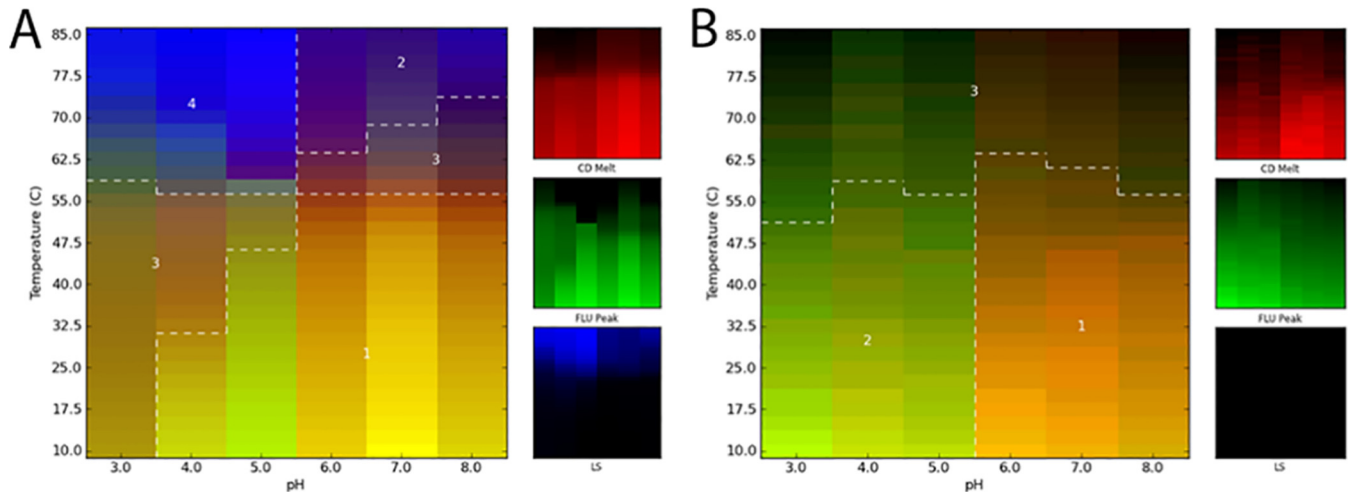


FIG 2 Biophysical characterization data for the DB fusion in the presence of OPOE (A to C) and LDAO (D to F). Far UV CD molar ellipticity at 222 nm was monitored as a function of temperature from 10 to 90°C (A and D). The intrinsic Trp fluorescence peak position wavelength (B and E) and light-scattering intensity were monitored at 295 nm as a function of temperature from 10 to 85°C (C and F). Error bars represent standard deviations from three different experiments. Symbols: pH 3, ■; pH 4, □; pH 5, ●; pH 6, ○; pH 7, ▲; pH 8, △.



**FIG 3** Three-index empirical phase diagram for DB fusion. EPDs were compiled from data collected in the presence of 0.5% OPOE (A) or 0.05% LDAO (B) that represented the conformational stability of the DB fusion as a function of pH and temperature (14).

At the initial 10°C temperature, the OPOE-DB fusion showed reduced secondary structure at acidic pHs compared to neutral pH. Independent of pH, the OPOE-DB fusion exhibited a thermal transition between 55°C and 59°C accompanied by a significant loss of secondary structure as the temperature was raised further. In contrast, the LDAO-DB fusion showed a lower degree of thermally induced structural alteration with little pH dependence. At 10°C, the intensity of the CD in the spectra recorded for the LDAO-DB fusion was lower than that for the OPOE-DB fusion. This difference suggested that the DB fusion is slightly unfolded in the presence of LDAO. A gradual, almost-linear increase then occurred without an apparent transition at acidic pH, with a small transition around 50°C apparent at neutral pH. Unlike the OPOE-DB fusion, the LDAO-DB fusion did not appear to completely unfold at higher temperatures, regardless of the pH. This lack of unfolding may be at least partially responsible for the ability to resist aggregation at high temperatures and the similarity of the CD spectra before and after exposure to higher temperatures during thermal melting (Fig. 1).

**LDAO leads to a more open, yet stable tertiary structure based on intrinsic Trp fluorescence.** Tertiary structure changes in the DB fusion in the presence of OPOE and LDAO were characterized by monitoring changes in intrinsic Trp fluorescence peak position wavelengths as a function of temperature and pH (Fig. 2B and E). The DB fusion contains five Trp residues, with four in IpaD and one in IpaB. The initial peak position of the OPOE-DB fusion at pH 3 was near 342 nm, which is consistent with partial exposure of indole side chains to more polar environments and the conformational alterations seen with CD spectroscopy in acidic environments (Fig. 3B). As the temperature was increased, a mild red shift appeared, followed by a thermally induced blue shift at 65°C. Peak positions of the OPOE-DB fusion at pH 4 to 8 were near or under 340 nm, suggesting that the Trp residues were less solvent exposed than at pH 3, although a steady increase in fluorescence emission wavelength was seen as a function of temperature, indicating enhanced exposure of Trp residues to a more polar environment. In general, the OPOE-DB fusion at pH 4 to 8 exhibited a transition at approximately 55 to 65°C, with a sharper transition observed at pH 5. Beyond the transition point, the tryptophans of the OPOE-DB fusion exhibited either a red or blue shift, depending on the pH, which was consistent with the aggregation that was confirmed by light scattering (see below).

In contrast to the OPOE-DB fusion, the Trp emission maxima of the LDAO-DB fusion at 10°C (Fig. 2E) were higher than 345 nm, suggesting that one or more of the indole side chains were only partially buried within the protein. As the pH increased, a gradual red shift occurred in all cases, indicating that the Trp residues were becoming more exposed to the aqueous environment. Regardless of pH, however, the peak position wavelength increased at the elevated temperature, indicating an even more open environment surrounding the Trp residues, but without any well-defined unfolding transitions. As seen with the CD thermal melts, this thermal resilience may be attributed to the maintenance of a more stable tertiary structure induced by LDAO that prevents aggregation.

**LDAO prevents protein aggregation as demonstrated by static light scattering.** Static light scattering measurements were performed simultaneously with collection of intrinsic fluorescence to examine the aggregation behavior of the DB fusion as a function of pH and temperature (Fig. 2C and F). The OPOE-DB fusion exhibited aggregation at a high temperature at all pH values examined. Aggregation onset at pH 3 to 5 was seen at around 35°C, while samples at pH 6 to 8 began to aggregate at 55°C. The protein precipitated and then started to settle out of solution at approximately 60°C for samples at pH 4 to 7 and around 70°C for samples at pH 3 and 8, which probably explains the decrease in emission signal seen after the transition in the intrinsic Trp fluorescence experiments (data not shown). The static light scattering data indicated that the DB fusion proteins in neutral environments exhibited the highest stability, which minimized their aggregation up to 55°C (Fig. 2C). No significant increase in light scattering was observed for the LDAO-DB fusion, regardless of temperature and pH, indicating no significant aggregation for this protein. These data were consistent with the results from intrinsic fluorescence, which showed no blue shift at temperatures up to 85°C (Fig. 2D).

**Empirical phase diagrams visually illustrate the resilience of the DB fusion in LDAO.** A data visualization approach, the three-

index EPD approach, was generated from the data sets obtained from far-UV CD, intrinsic Trp fluorescence, and static light scattering as a function of temperature and pH for the DB fusion in the presence of OPOE or LDAO. In the three-index EPDs, different colors were assigned to the changes in different protein structural states. Red was assigned to the secondary structure (molar ellipticity at 222 nm), green to the tertiary structure (Trp fluorescence peak position wavelength), and blue to the quaternary structure or aggregation (light scattering intensity at 295 nm). The comparative EPDs are shown in Fig. 3.

The EPD of the OPOE-DB fusion can be divided into four apparent regions (Fig. 3A). Region 1 is the yellow area covering pH 6 to pH 8 below 55°C, pH 5 below 45°C, and pH 4 below 30°C. It represents the conditions in which the protein is in its most stable, native-like form. In region 2, the dark color denotes samples in a highly structurally altered state (secondary and tertiary structures are partially lost) with a lower degree of aggregation compared to region 4. Region 3 depicts the protein in a less partially unfolded state, either due to relatively a high temperature at pH 6 to 8 or due to an acidic environment. Blue region 4 represents aggregation of the proteins at acidic pH and high temperature. Overall, the OPOE-DB fusion is maintained in its most stable state at neutral pH and below 55°C.

The three-index EPD of the LDAO-DB fusion exhibited a pattern distinct from that of the OPOE-DB fusion (Fig. 3B). As temperature increased, all measurements (except static light scattering, which showed no change) showed gradual and constant changes without sharp color divisions. Since there was no drastic change, the clusters were limited to the area of higher temperatures for all pH values and acidic or neutral pH for lower temperatures. Data at pH 3 to 5 indicated a more apolar microenvironment around Trp residues (fluorescence peak position) and less secondary structure (CD) than at pH 6 to 8 at lower temperatures. It is important to note, however, that no aggregation was observed at any pH or temperature tested when the DB fusion was in the presence of LDAO. Again, there was no evidence for any thermal transitions, because the LDAO-DB fusion essentially remained in a structural state that was similar to that at 10°C. This is in stark contrast to the results with the OPOE-DB fusion, which lost structure and aggregated above ~60°C. Thus, LDAO appears to confer a thermal plasticity or resilience to the DB fusion by which, at lower temperatures, the protein maintains a structure that may be considered slightly more open, while at higher temperatures it does not completely unfold.

**LDAO elicits a higher IL-17A response and gives rise to protection from lethal challenge by *Shigella*.** To determine the impact of the biophysical differences observed with LDAO on the efficacy of the DB fusion as a subunit vaccine, we immunized mice intranasally with 20 µg of DB fusion in each of the detergents admixed with the adjuvant dmLT. Antibody titers specific for IpaB or IpaD showed no significant differences regardless of which detergent was used (Fig. 4A and B). Higher levels of IL-17A secretion, however, were observed when splenocytes obtained at day 56 from animals immunized with the LDAO-DB fusion were stimulated with IpaD, while the IpaB-specific IL-17A response was similar for each protein preparation (Fig. 4C). Because IpaB and IpaD are potential protective antigens by themselves, this increased stimulation of IpaD-specific IL-17A was considered of potential importance, since IL-17A has been associated with protection from *S. flexneri* (8). Measurement of other cytokines did

not reveal any differences in responses to stimulation with the antigens (data not shown).

Because *Shigella* spp. only infect humans and nonhuman primates, mice or other small animals do not contract shigellosis or exhibit any of the hallmark symptoms. The accepted model is a lethal pulmonary model where the pathogen is introduced into the lung via the nose and the animals exhibit symptoms of and succumb to pneumonia (15). Thus, when animals immunized with the DB fusion were then challenged with a very high dose of virulent *S. flexneri* 2457T, the mice that received the LDAO-DB fusion showed significantly higher survival than mice that received the OPOE-DB fusion ( $P < 0.05$ , log rank test) (Fig. 5). Control mice that received PBS or PBS containing the dmLT adjuvant alone failed to survive the challenge.

## DISCUSSION

While research has focused on the development of live, attenuated vaccines against *Shigella* spp., such vaccines have the disadvantage of typically evoking serotype specificity due to skewing the host immune response toward surface lipopolysaccharide (LPS). A subunit vaccine composed of the DB fusion, a fusion of the IpaD and IpaB proteins, provides an advantage in that it is composed of highly conserved T3SS components, which means that it can protect against all serotypes, since the T3SS is a required virulence factor for all *Shigella* spp. Furthermore, it is likely to have a better safety profile, since it is a defined recombinant protein and has the potential advantage of reduced reactogenicity since it contains no bacterial LPS. Similarly, the DB fusion does not require oral administration by a target population (which is typically malnourished and possesses a gut flora substantially different from the trial population of the developed world). Initial vaccine efficacies in mice were determined with the DB fusion in OPOE, a detergent that is used to remove the chaperone and maintain the DB fusion in a soluble state. Unfortunately, OPOE is an expensive detergent that has no record of use in human products. LDAO, a much less expensive detergent, was substituted here based on previous success with it and IpaB (9). It is a well-defined detergent that has a GRAS profile, having been used in facial creams. As previously seen with IpaB, LDAO caused the release of IpgC from the DB fusion while also preventing oligomerization and thermally induced aggregation of the DB fusion.

In this work, the conformational stability of the DB fusion in OPOE or LDAO was extensively characterized by employing a variety of methods. Far-UV circular dichroism, intrinsic tryptophan fluorescence, and static light scattering were used to monitor the DB fusion structure at the secondary, tertiary, and quaternary levels as a function of temperature and pH. The resulting large data set was summarized into three-index EPDs to visualize the collective protein structural changes that occurred in response to changes in environmental conditions. A unique EPD was generated for the DB fusion in each detergent. The OPOE-DB fusion lost much of its secondary and tertiary structures as a result of thermal stress, regardless of pH. The loss of structure resulted in aggregation and the formation of insoluble precipitates. The EPD of the OPOE-DB fusion showed that it was most stable at pH 6 to 8, with unfolding occurring at lower pH and higher temperature and complete aggregation after 60°C at pH 3 to 5. In contrast, while the LDAO-DB fusion exhibited reduced compact secondary and tertiary structures relative to the OPOE-DB fusion, little loss of structure was seen upon thermal stress, independent of pH.

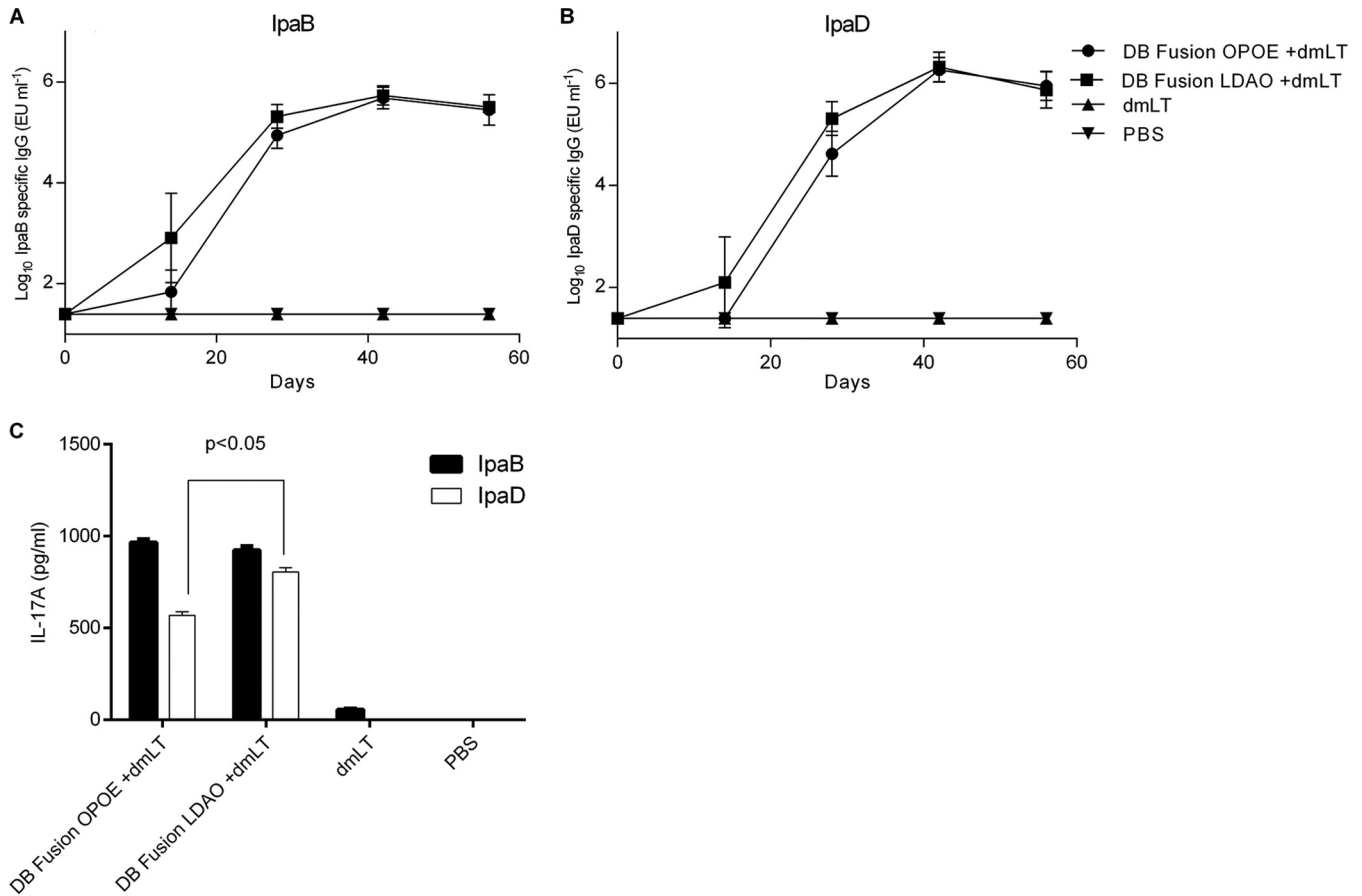


**FIG 4** Immunogenicity after immunization with DB fusion in OPOE or LDAO. Mice ( $n = 10$  per group) were immunized intranasally with OPOE-DB fusion or LDAO-DB fusion admixed with dmLT at days 0, 14, and 28. Blood samples were collected, and serum antibody titers against IpaB (A) or IpaD (B) were determined individually via an ELISA. Spleen cells obtained from immunized mice were stimulated with IpaB or IpaD. The IL-17A levels in the resulting cell supernatants were determined in an ELISA (C).

Furthermore, no aggregation was observed at any temperature or pH tested. It is perhaps even more impressive that the protein secondary structure appears to return to its original state after heating to temperatures as high as 90°C and cooling back to 10°C. Taken together, these results suggest that the DB fusion in LDAO is in a very distinctive state which provides the protein an element

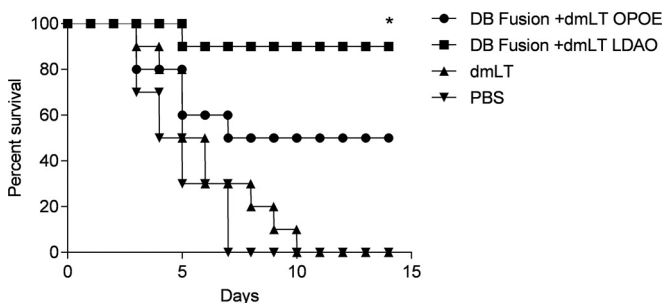


**FIG 5** Survival of mice vaccinated with DB fusion after challenge with *S. flexneri*. Mice ( $n = 10$ ) immunized intranasally with 20  $\mu$ g DB fusion in OPOE or LDAO with dmLT were challenged with  $1.6 \times 10^7$  CFU of *S. flexneri* 2457T delivered intranasally. Animals that received dmLT alone or PBS alone were included as negative controls. Survival was monitored for 14 days. \*,  $P < 0.05$ , log rank test, versus DB fusion plus dmLT in OPOE.

of elasticity and an ability to adapt to more extreme pH and temperature conditions. It is possible that the LDAO, being a non-denaturing zwitterionic surfactant, interacts with charged protein residues on the protein surface, which in addition to elasticity also reduces oligomerization and deleterious aggregative processes. In contrast, OPOE is a heterogeneous nonionic detergent with a single polar hydroxyl group in the head groups with dispersed ether linkages and is likely to only be able to interact with the hydrophobic regions of the IpaB portion of the DB fusion and thus not protect the protein from aggregation (9). Although the experiments with LDAO were conducted at a 10-fold-lower concentration, this lesser amount of LDAO was still able to act in a similar fashion to OPOE in terms of removal of the complexed chaperone and its solubilization ability.

Because LDAO has the ability to mildly influence the solution structure of the DB fusion and dramatically alter the solution properties of this candidate vaccine under extreme conditions, it was deemed necessary to assess potential changes that LDAO may cause in immunogenicity. This is especially true since the LDAO-DB fusion is predominantly a monomer, and previous studies have shown that multimeric antigens tend to induce better memory immune responses than monomeric antigens (16). In the case of the DB fusion, we have shown that some immune re-

sponses, such as Th17-associated cytokine levels (IL-17A), are higher when the protein is delivered in LDAO. This is not, however, the result of an overall higher immune response, because the levels of antibodies (IgG) specific to IpaB or IpaD are not distinguishable from the DB fusion delivered with OPOE. This suggests that some cell-mediated immune responses are elevated when the folding/multimeric state of the protein is altered by LDAO. The relevance of these responses were highlighted in the challenge experiment, since the protein in LDAO provided higher survival/protection levels than the protein in OPOE. This result emphasizes the importance of optimizing the vaccine formulation for this protein.

The development of the novel recombinant DB fusion protein as a *Shigella* vaccine candidate represents a unique platform for providing a broadly protective and affordable vaccine for children in low-income countries. This reformulation study identifies LDAO as a detergent that enables the DB fusion to exhibit greater plasticity and resistance to the permanent effects of pH and temperature extremes than seen under the conditions (i.e., preparation in OPOE) previously defined. This could facilitate less dependence on the vaccine cold chain in the ultimate distribution of the vaccine. While overall conceptually intriguing, the most important outcome of these biophysical characterizations is that LDAO was found to significantly stabilize the DB fusion over previous conditions, which resulted in the prevention of protein aggregation. Aggregation is an undesirable property in vaccine formulations due to the loss of efficacy and increased instability. Furthermore, this revised formulation resulted in increased IL-17A responses, which may lead to increased vaccine efficacy. The structural and immunogenic principles behind these phenomena will now require further investigation to determine if and how they are linked.

## ACKNOWLEDGMENTS

This work was funded by a grant from PATH-EVI to W.L.P., from National Institute of Allergy and Infectious Diseases of the National Institutes of Health under award number R01 AI113307 to W.L.P. and R01 AI99489 to W.D.P., and internal funding for the Macromolecule and Vaccine Stabilization Center of the University of Kansas.

The content is solely the responsibility of the authors and does not necessarily represent the official views of the NIH or PATH-EVI.

## REFERENCES

- Kotloff KL, Nataro JP, Blackwelder WC, Nasrin D, Farag TH, Panchalingam S, Wu Y, Sow SO, Sur D, Breiman RF, Faruque AS, Zaidi AK, Saha D, Alonso PL, Tamboura B, Sanogo D, Onwuchekwa U, Manna B, Ramamurthy T, Kanungo S, Ochieng JB, Omoro R, Oundo JO, Hossain A, Das SK, Ahmed S, Qureshi S, Quadri F, Adegbola RA, Antonio M, Hossain MJ, Akinsola A, Mandomando I, Nhampossa T, Acacio S, Biswas K, O'Reilly CE, Mintz ED, Berkeley LY, Muhsen K, Sommerfelt H, Robins-Browne RM, Levine MM. 2013. Burden and aetiology of diarrhoeal disease in infants and young children in developing countries (the Global Enteric Multicenter Study, GEMS): a prospective, case-control study. *Lancet* 382:209–222. [http://dx.doi.org/10.1016/S0140-6736\(13\)60844-2](http://dx.doi.org/10.1016/S0140-6736(13)60844-2).
- Schroeder GN, Hilbi H. 2008. Molecular pathogenesis of *Shigella* spp.: controlling host cell signaling, invasion, and death by type III secretion. *Clin Microbiol Rev* 21:134–156. <http://dx.doi.org/10.1128/CMR.00032-07>.
- Abrusci P, McDowell MA, Lea SM, Johnson S. 2014. Building a secreting nanomachine: a structural overview of the T3SS. *Curr Opin Struct Biol* 25:111–117. <http://dx.doi.org/10.1016/j.sbi.2013.11.001>.
- Martinez-Becerra FJ, Kissmann JM, Diaz-McNair J, Choudhari SP, Quick AM, Mellado-Sanchez G, Clements JD, Pasetti MF, Picking WL. 2012. Broadly protective *Shigella* vaccine based on type III secretion apparatus proteins. *Infect Immun* 80:1222–1231. <http://dx.doi.org/10.1128/IAI.06174-11>.
- Martinez-Becerra FJ, Scobey M, Harrison K, Choudhari SP, Quick AM, Joshi SB, Middaugh CR, Picking WL. 2013. Parenteral immunization with IpaB/IpaD protects mice against lethal pulmonary infection by *Shigella*. *Vaccine* 31:2667–2672. <http://dx.doi.org/10.1016/j.vaccine.2013.04.012>.
- Heine SJ, Diaz-McNair J, Andar AU, Drachenberg CB, van de Verg L, Walker R, Picking WL, Pasetti MF. 2014. Intradermal delivery of *Shigella* IpaB and IpaD type III secretion proteins: kinetics of cell recruitment and antigen uptake, mucosal and systemic immunity, and protection across serotypes. *J Immunol* 192:1630–1640. <http://dx.doi.org/10.1049/jimmunol.1302743>.
- Martinez-Becerra FJ, Chen X, Dickenson NE, Choudhari SP, Harrison K, Clements JD, Picking WD, Van De Verg LL, Walker RI, Picking WL. 2013. Characterization of a novel fusion protein from IpaB and IpaD of *Shigella* spp. and its potential as a pan-*Shigella* vaccine. *Infect Immun* 81:4470–4477. <http://dx.doi.org/10.1128/IAI.00859-13>.
- Sellge G, Magalhaes JG, Konradt C, Fritz JH, Salgado-Pabon W, Eberl G, Bandeira A, Di Santo JP, Sansonetti PJ, Phalipon A. 2010. Th17 cells are the dominant T cell subtype primed by *Shigella flexneri* mediating protective immunity. *J Immunol* 184:2076–2085. <http://dx.doi.org/10.4049/jimmunol.0900978>.
- Dickenson NE, Choudhari SP, Adam PR, Kramer RM, Joshi SB, Middaugh CR, Picking WL, Picking WD. 2013. Oligomeric states of the *Shigella* translocator protein IpaB provide structural insights into formation of the type III secretion translocon. *Protein Sci* 22:614–627. <http://dx.doi.org/10.1002/pro.2245>.
- Schuck P. 2000. Size-distribution analysis of macromolecules by sedimentation velocity ultracentrifugation and Lamm equation modeling. *Biophys J* 78:1606–1619. [http://dx.doi.org/10.1016/S0006-3495\(00\)76713-0](http://dx.doi.org/10.1016/S0006-3495(00)76713-0).
- Laue TM, Shah BD, Ridgeway TM, Pelletier SL. 1992. Computer-aided interpretation of analytical sedimentation data for proteins, p 90–125. *In* Harding SE, Rowe AJ, Horton JC, Analytical ultracentrifugation in biochemistry and polymer science. Royal Society of Chemistry, Cambridge, United Kingdom.
- Lebowitz J, Lewis MS, Schuck P. 2002. Modern analytical ultracentrifugation in protein science: a tutorial review. *Protein Sci* 11:2067–2079. <http://dx.doi.org/10.1110/ps.0207702>.
- Garcia de la Torre JG, Bloomfield VA. 1981. Hydrodynamic properties of complex, rigid, biological macromolecules: theory and applications. *Q Rev Biophys* 14:81–139. <http://dx.doi.org/10.1017/S0033583500002080>.
- Kim JH, Iyer V, Joshi SB, Volkin DB, Middaugh CR. 2012. Improved data visualization techniques for analyzing macromolecule structural changes. *Protein Sci* 21:1540–1553. <http://dx.doi.org/10.1002/pro.2144>.
- van de Verg LL, Mallett CP, Collins HH, Larsen T, Hammack C, Hale TL. 1995. Antibody and cytokine responses in a mouse pulmonary model of *Shigella flexneri* serotype 2a infection. *Infect Immun* 63:1947–1954.
- Ogun SA, Dumon-Seignover L, Marchand JB, Holder AA, Hill F. 2008. The oligomerization domain of C4-binding protein (C4bp) acts as an adjuvant, and the fusion protein comprised of the 19-kilodalton merozoite surface protein 1 fused with the murine C4bp domain protects mice against malaria. *Infect Immun* 76:3817–3823. <http://dx.doi.org/10.1128/IAI.01369-07>.